Journal of Applied Polymer Science

Beneficial Role of "Sol-Gel" Synthesized Mesoscale Silica Networks on the Performance of Liquid Silicone Elastomer†

Anubhav Saxena,[1] Debarshi Dasgupta,[1] Shreedhar Bhat,[1] Sandip Tiwari,[1] Laxmi Samantara,[1] Dieter Wrobel[2]

[1]Global Research and Development Center, Momentive Performance Materials Pvt. Ltd, Survey # 9, Electronic City West (Phase 1), Bangalore 560100, India

[2]Research and Development Center, Momentive Performance Materials GmbH, 51368 Leverkusen, Germany

Correspondence to: A. Saxena (E-mail: Anubhav.Saxena@momentive.com)

†Dedicated to Prof. Michiya Fujiki on the occasion of his 60th birthday.

ABSTRACT: This piece of contribution highlights the profound effect of unique mesoscale morphology of tailor made nanosilica assembly (SS-Silica), synthesized by sol–gel route, on the mechanical and dynamic rheological properties of platinum catalyzed addition-cured silicone elastomers. While commercial colloidal nanosilica (CS Silica) is used as the control nanofiller representing particulate morphology, the tailor-made SS-Silica having highly percolated network structure offers 10-fold increase in storage modulus of the uncured reactive PDMS precursor nanocomposite with stable dynamic rheological behavior and more than 180% enhancement in tensile strength of resulting liquid silicone rubber (LSR) produced on curing, as compared to colloidal silica of commercial origin. © 2013 Wiley Periodicals, Inc. J. Appl. Polym. Sci. **2014**, *131*, 40125.

KEYWORDS: elastomers; morphology; crosslinking

Received 24 July 2013; accepted 26 October 2013
DOI: 10.1002/app.40125

INTRODUCTION

Elastomers are a unique class of engineered materials exhibiting high reversible deformation under mechanical stress with distinctly low elastic modulus. Such property arises due to the presence of highly flexible polymer chains (due to low interchain interactions) in combination with crosslinked structure which prevents sliding of chains against their immediate neighbors causing plastic flow.[1–3]

In comparison to synthetic organic elastomers, "silicone" [chemically they are poly(dimethyl siloxane); PDMS based macromolecules] elastomers have gained much industrial attentions owing to excellent weatherability, extended thermal stability (i.e., very wide operating temperature window), ultralow temperature toughness, good dielectric properties, low surface energy (surface tension = 20.4 mN m^{-1}), high biocompatibility and optical transparency. Silicone elastomers are widely used in various applications such as sealants, adhesives, high voltage insulation (HVI) devices, electronics (RTV elastomers), automotive, and healthcare.[4–8] The enhanced stability of poly(dimethyl siloxane) polymers is mainly attributed by higher Si—O bond energy (445 kJ mol^{-1}) as compared to that of C—C bond (346 kJ mol^{-1}). Moreover, owing to very high rotational entropy (low rotational energy barrier around Si—O bond viz. 0.2 kJ $mole^{-1}$) PDMS has exceptionally low glass transition temperature (146 K) resulting high degree of flexibility in and around the chains. By design, silicone elastomers are thermo-setting polymers synthesized by curing of reactive poly(dimethyl siloxane) (PDMS) gums with polysiloxane based crosslinkers. More often, the curing chemistry involves thermal or photo induced hydrosilylation reactions promoted by platinum based catalysts in particular Pt (0) complexes such as Karstedt's catalyst, for its stability and compatibility with silicones.[9–13]

However, a crosslinked PDMS network cannot alone qualify on the mechanical robustness required for good elastomeric application and henceforth, reinforcing fillers are compounded prior to thermoset formation. The reinforcement happens due to hydrodynamic effect imported by the rigid fillers as well as by polymer-filler bonding.[14–16] Although, a variety of high aspect-ratio nanofillers have been investigated in silicone elastomer matrices,[17–19] so far, silica structures have been mostly used in industrial scale to reinforce silicone elastomers, as they can simultaneously offer high structural resemblance

Additional Supporting Information may be found in the online version of this article.

(compatibility), improved stress bearing ability, higher heat tolerance and most importantly higher optical transmissibility.[20–24] The only concern with inherently hydrophilic silica fillers (due to the presence of peripheral silanolic groups) is the strong filler–filler interaction due to hydrogen bonding between peripheral hydroxyls[25] which can be evaded by surface treatment with silane capping agents. It is worth mentioning here, that a fraction of reactive hydroxyl groups on silica surfaces is rather beneficial to promote polymer–filler adhesion, but it always appears to be challenging to mask the hydroxyl function partially to have exact control on both phenomena. Thus, to take advantage of hydrogen bond mediated association[26–28] of silica with PDMS chains, the hydrophobization of silica surface is purposefully performed only partially. This also attributes to lesser filler–filler agglomeration and mitigates the possibilities of occurring "creep hardening" effect.[14–16]

The properties (c.a., thermal, mechanical) of the final silicone elastomers greatly depend on the silica types (more specifically the filler aspect ratio, bulk filler morphology and/or polymer–filler interface chemistry) used to formulate the nanocomposite. The silica particles often employed in such functional materials are hydrated, precipitated, colloidal and fumed silica. Colloidal silica (named as CS–silica in what follows) particles are produced through sol–gel chemistry by hydrolysis of alkali metal silicates or silicon alkoxide to silicic acid, which rapidly self-condense under the experimental condition to form polysilicic acid structure. The morphology of colloidal silica particles is characterized as more discrete particle formation with specific surface area higher than that of precipitated silica. These particles are typically spherical in nature with diameter varying from 15 nm to ~100 nm.[29,30] Unevenly distributed particle aggregates formation in the nanocomposite can be avoided to some extent by the surface treatment of silica. Silica surface-modification effects on polymer adsorption characteristics as a function of surface coverage. The appropriate surface functionalization of the silica particles can result in precise control of the silica morphology and the final properties of the composite elastomer. However, the lack of interconnectedness between the fillers limits the reinforcement and rheological benefits compared to fumed silica,[31] where interconnected silica structures are produced by an exhaustive process involving flame pyrolysis of silicone tetrachloride. When immobilized in an aprotic medium, the fumed silica aggregates to form a continuous three-dimensional network over the mesoscale length by interacting between themselves through interparticle hydrogen bonds. However, the presence of silanol groups on the nascent fumed silica particulates leads to a strong filler–filler interaction giving rise to a high irreversible filler agglomeration inside the cured rubber matrix and, hence, the difficulty in processing and scale up. To overcome this creep hardening effect, it needs an additional post treatment steps to silylate a fraction of surface —OH functionality in combination with the tedious and meticulous synthetic process of fumed silica.[31]

To mitigate these process related issues, we have come up with a mild sol–gel synthesis method to create an alternative three-dimensional network of nanosilica filler. The advantage here is really two folds. Benefit of effective stress distribution through percolated filler network is achieved without much compromise with safe operation procedure by avoiding use of any form of particulate dispersion and additional surface modification.

Therefore, synthetic silica's have been developed to take advantage of uniform morphology to provide specific benefits to the elastomer formulators. A novel protocol to *in situ* functionalized nanosized silica particles by sol–gel method using silane as a capping agent has been reported by us previously.[32] The silica particles prepared using this methodology has been shown to improve storage and dispersion stabilities. The present study explores the use of morphological aspects of silica nanofillers in controlling the mechanical properties of liquid silicone rubber (LSR) at different dispersion levels against the commercial colloidal silica particles. The present study also highlights the effect of nanofiller morphology on the silicone elastomer reinforcement. The experimental observations of the present study are detailed in the proceeding sections.

EXPERIMENTAL

Materials

Vinyl-terminated linear polydimethylsiloxane (PDMS) (Viscosity of 65 Pa.s), hydrogen-siloxane fluid, and hexamethyl-disilazane (HMDZ) were obtained from Momentive Performance Materials, USA and used as received. Sodium silicate solution and ethyl alcohol were purchased from Aldrich chemicals. Thermax T-63, an acidic ion exchange resin, was purchased from Tulsion. Reference filler, colloidal silica, was obtained from Nalco and was post functionalized using HMDZ.

Synthesis of Silica Nanoparticles by Sol–Gel Method

Thermax T-63 ion exchange resin (IER) (13.4 g) was mixed with water (30 mL, Milli Q) in a 250-mL beaker. Sodium silicate solution (13.3 mL) was taken in a 500 mL three-necked round bottomed flask and water (10 mL) was added to it. The IER dispersion was transferred to sodium silicate solution at room temperature with stirring. The stirring was continued for 1 h. The solution was filtered soon after the pH drops down to ~9. To the filtrate, with stirring, was added ammonia solution (2 mL) and the solution was warmed to 60°C. Then HMDZ (6 mL in 20 mL ethanol) was added drop-wise for 5 min and the stirring was continued for additional 90 min. Heating was stopped followed by the addition of ethanol (50 mL) with continuous stirring for 1 h. An additional amount of ethanol (20 mL) was added and the stirring was continued for another 30 min. The final silica dispersion was optically translucent and stable under ambient conditions with no gelation.

Synthesis of Silica-reinforced Poly(dimethyl siloxane) Nanocomposites and Elastomer Containing Silica Nanoparticles (LSR)

Silica–poly(dimethylsiloxane) composite was prepared by mixing the silica dispersions, and vinyl terminated PDMS, using planetary mixer. Water, ethanol and other volatiles in the mixture were stripped off at 80°C, under vacuum. The nanocomposite was mixed with a hydrogensiloxane fluid (a cross-linker), Karstedt's Catalyst and ethyl cyclohexenol (ECH), an inhibitor, using a hand blender. The blended mixture was placed in a mold and cured at 165°C for 10 min using compression-molding equipment to obtain a 2-mm thick silicone rubber

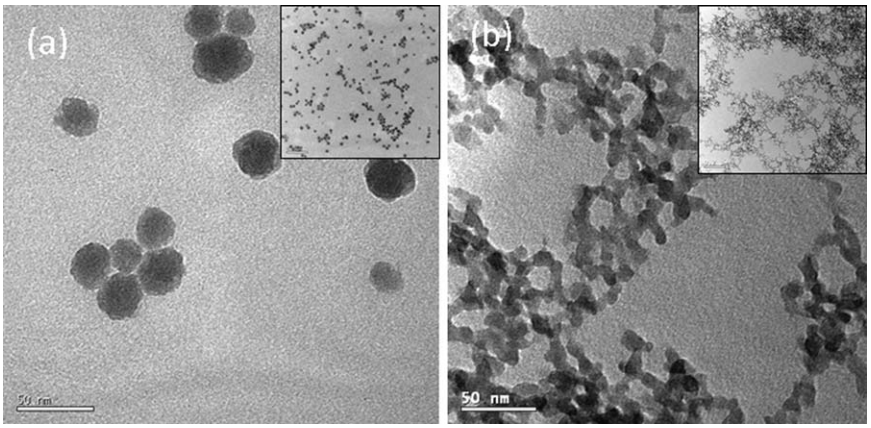

Figure 1. (a) TEM image of colloidal silica (CS_Silica) particles in the dried form before dispersion: the inset picture corresponds to the same grid showing low magnification TEM image (scale bar = 50 nm). (b) TEM image of Sol-Gel nanosilica (SS_Silica) particles in the dried form before dispersion: the inset picture corresponds to the low magnification TEM image (scale bar = 50 nm).

sheets. Using this protocol, 17, 20, and 24 wt % silica–poly (dimethylsiloxane) nanocomposite were produced and cured thereafter using compression molding equipment.

Material Characterization

The hydrophobic nanosilica was characterized using Fourier Transform Infra-red (FTIR) Spectrophotometer (Perkin Elmer), solid state ^{29}Si NMR (79.5MHz, Bruker) and thermo gravimetric analysis (TGA).[32] For TGA, the sample was heated from 25°C to 700°C at a heating rate of 10°C per minute on a TGA 2950 (TA instruments). The size and morphology of the functionalized silica particles were analyzed using Technai G2 transmission electron microscopy (TEM) instrument. The silica dispersed uncured LSR formulation was characterized by rheology using an RDA III strain controlled Rheometer.

The mechanical strengths (tensile strength, elongation and modulus etc.) of the cured silicone rubber sheets were characterized using an Instron 3356 tensile tester at room temperature (25°C). Sample dimensions and testing procedure were in accordance with DIN 53504. The gauge length of the specimens was 4 mm × 2 mm. The crosshead speed was 200 mm min^{-1}. All measurements were repeated five times and the values averaged. The Young's modulus was determined from the initial slope of stress–strain curve.

The hardness of elastomer sheets was measured by Shore A REX GAUGE durometer, which is a portable device that uses a truncated cone indenter point and a calibrated steel spring to measure the resistance of the elastomer to indentation.

The DLS experiments were carried out with a 0.1 wt % SS-Nanosilica "sol" using Viscotek 802 DLS was measured in quartz cuvette of optical path length 3 mm. The recorded data were analyzed by OmniSize software

RESULTS AND DISCUSSION

The particle morphologies of the commercial colloidal silica (designated as CS, post functionalized with tri-methylsilyloxy) and synthesized sol–gel nanosilica (prepared by sol–gel process as explained in the materials section, designated as SS sample in what follows) were characterized by transmission electron microscopy (TEM). The TEM images of the respective silica particles are shown in Figure 1(a,b). The images seen for air-dried samples revealed an interconnected network like morphology for sol–gel silica (formed at solid air interface) compared to distinctly isolated nearly spherical particles of commercial colloidal silica. The individual particle sizes observed for the sol-gel silica (as measured from the network structure) are in the range of 10–15 nm [Figure 1(b); although no isolated particle exists] whereas, the average particle diameter for CS particles measures 25 ± 3 nm [Figure 1(a)] as revealed under TEM. The inset of Figure 1(a) shows the global bulk morphology of CS–silica which is mostly discrete in distribution with some random colonies those, might form due to solvent drying during dispersion deposition on the TEM grid.

However, the particle size analysis of the SS–silica nanostructure using dynamic light scattering (DLS) (see Supporting

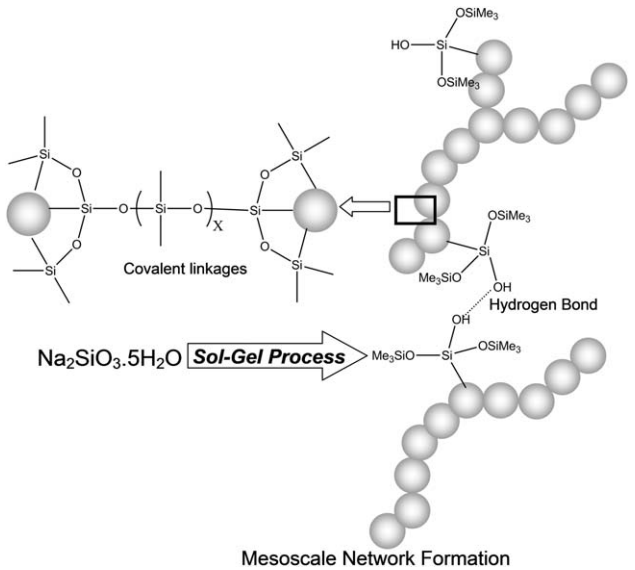

Figure 2. Schematic Illustration of formation mechanism of SS nanosilica synthesis and self-assembly to yield percolated network.

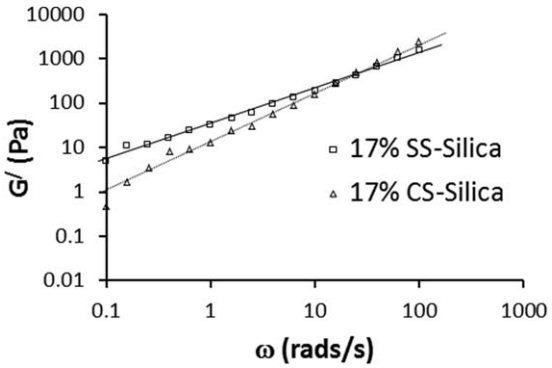

Figure 3. Rheological mapping of polymerizable PDMS/silica nanocomposite reinforced with indicated type of nanofillers at 17% (w/w) loading.

Information file Figure S1) indicates a wider distribution ranging from 10 to 100 nm. In the dispersed state, this SS–silica seems to retain the network structure as seen in TEM yielding higher hydrodynamic volume in DLS. This observation supports the network structure observed on TEM of SS–silica even in the hydrated state. While the inset of Figure 1(b) clearly demonstrates that the percolated network formed by SS–silica is of length scale of few hundreds of nanometer thus, re-emphasizing the fairly long range "meso-scale" ordering.

Figure 2 illustrates plausible formation route of SS silica network structure through cooperative self-assembly. It is also anticipated that the silane capping agent HMDZ used, efficiently screen a fraction of uncondensed hydroxyl groups originally present on the particle surfaces. ^{29}Si NMR (see Supporting Information file Figure S2) of the SS–silica indicates the presence of Q, and M Silicon atoms (Q is named when Si is attached to four neighboring oxygen atoms and M when Si is linked with only one oxygen atom). A broad Q ^{29}Si peak (around −100 ppm) is attributed by silica network whereas M peak (at + 12 ppm) is the signature of trimethyl-silyl capping resulted from HMDZ *in situ* functionalization.[32]

These hydrophobic silane groups present on the silica surface would help particles to compatibilize better on the PDMS chains during the elastomer compounding and the residual pendent silanol groups would provide synergistic polymer–filler interaction. The state of the art here is truly the delicately balanced filler–polymer and filler–filler interactions within the polymerizable PDMS matrix which would ultimately provide the reinforced mechanical properties of the resulting LSR material. It is worth stressing here that, trimethyl-silyl functionalization of CS–silica obtained from commercial source could not produce the typical interconnected meso-scale association as is concluded from TEM studies.

Physically blended silica nanofiller/reactive PDMS (hydride and Vinyl) nanocomposites were investigated for rheological properties prior to curing. For both of the kinds of silica nanofiller loaded at 17% (w/w), loss moduli dominate over the storage moduli [see Supporting Information file Figure S3(a,b)], however, SS–silica nanocomposite measures higher storage modulus as compared to that of CS–silica over the entire frequency regime, (Figure 3) indicating significant reinforcement by the former. Moreover, the fact that the slope of storage modulus vs. oscillation frequency is less for SS–silica nanocomposite also refers to the more structured nature of the SS–silica hybrid. When the loading was increased to 20% (w/w), and furthermore to 24% (w/w), the liquid like behavior is slowly diminishing and the solid like structure starts building up.

In the frequency sweep experiment [Figure 4(a,b)], it is evident that the storage modulus (G') is increased significantly with higher loading (at 20% w/w) of the sol–gel silica [in the range of 10^4 Pa; see Figure 4(b)] compared to colloidal silica [10^3 Pa; see Figure 4(a)]. Moreover, at 20% (w/w) filler loading, the structure build-up was seemingly more pronounced in sol–gel silica-poly(dimethylsilioxane) nanocomposites as the $G' \propto \omega^n$ and the exponent "n" is notably lower for SS–silica nanocomposite over CS–silica. It is anticipated that the structuration of the material comes from a synergistic effect involving increased surface contacts by the adsorption of the silanized silica surface on the poly(dimethylsiloxane) chains and superior stress distribution throughout the assembled mesoscale network.

For commercial colloidal silica particles, at 17, 20, and 24% (w/w) loading on poly(dimethylsiloxane), the structure build up was less pronounced [Figure 4(a)]. The material has been found to have higher viscous character at all loadings of the silica particles. Although, the structure build up observed is weak (10 fold lesser as compared to SS–nanosilica composite), the particle–particle interaction seems to play a major role in the material by flocculation. Hence, the observed enhancement in the G' is most likely

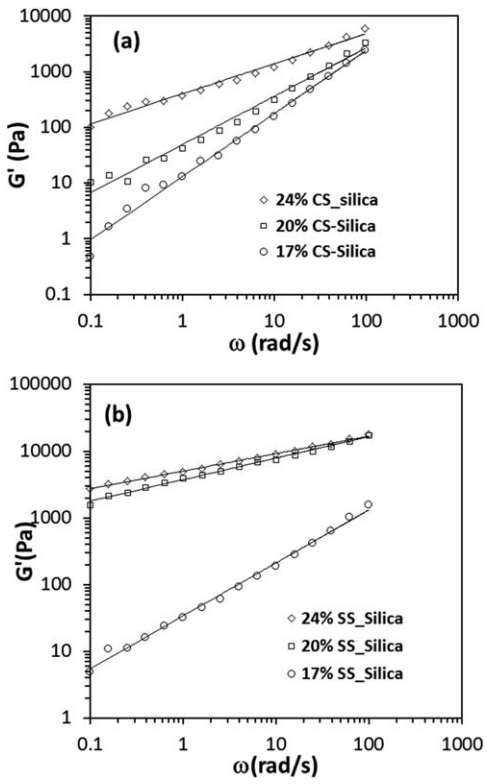

Figure 4. A plot of storage modulus (G') vs. Oscillation frequency (ω) at different filler loadings (w/w) for (a) CS–silica and (b) SS–silica as indicated.

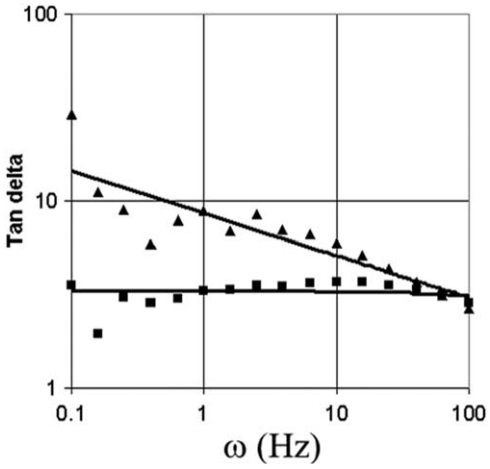

Figure 5. Tan-delta curves for CS (solid triangle) and SS (solid square) silica/polysiloxane composites.

due to the formation of particle aggregates and not because of enhanced filler–polymer dispersion.

This phenomenon can further be confirmed by looking at the tan δ versus frequency plots (Figure 5), also often, referred to as the consistency spectrum of the materials which indicates that the silica dispersion made from colloidal silica is not very stable and the viscoelastic character varies remarkably as the frequency of oscillation is increased. This observation is mainly due to the agglomeration of the CS–silica particles at larger frequency of oscillation, thus leading to polymer–filler phase separation even though containing same compatibilizer on their surfaces. However, the nanocomposite obtained from sol–gel silica retained its viscoelastic behavior constant over the entire shear frequency ranges tested. Therefore, sol–gel silica-poly(dimethylsiloxane) nanocomposite has more stable structure than that of colloidal silica with better polymer–particle compatibilization.

To explore further the effect of formulation additives on the processability of these elastomeric nanocomposites, the variation of complex viscosity with frequency of oscillation [presented in Supporting Information Figure S4(a,b)] is investigated. It is envisaged that the composite materials derived from SS–silica exhibit stronger shear thinning at relatively higher filler loading on a polymerizable PDMS matrix which clearly indicates that in SS–nanosilica, along with chemical bonds filler network also consists of reversible (physical) linkages.

Silica–Poly(dimethylsiloxane) Nanocomposites Elastomer

The potential application of such nanohybrids, composed of reactive PDMS, is to formulate liquid silicone rubber for advanced elastomeric performance. This prompted us to explore the effect of filler morphology on the LSR properties. The silica dispersed vinyl terminated poly(dimethylsiloxane), both sol–gel and colloidal, at different loadings (17, 20, and 24% w/w) were cured using standard compression molding technique to obtain liquid silicone rubber (LSR) nanocomposites. The material compositions were mostly kept essentially the same as those of uncured hybrids studied for dynamic rheological measurements, but additionally the ppm level of catalyst and inhibitor were added. These elastomer sheets are visually homogeneous and optically transparent. The hardness and mechanicals properties were analyzed by standard ASTEM or DIN test protocols.

The mechanical properties of the heat cured elastomer sheets were studied by tensile tester. The applied linear stress was plotted against the developed strain to understand the strength of the materials. The stress–strain curves indicated that the silica dispersed LSR samples store and dissipate mechanical energy very well. The material has significant elongation character and experimentally qualifies as an elastomer. The initial stress–strain response (as exhibited in the Supporting Information file Figure S5) is linear as it deforms and reforms to original shape after stress removal (Hookean solid). The slope calculated from the linear portion of the curve provided information related to stiffness of the material (known as the Young's modulus or the modulus of elasticity). With filler loading of 17% (w/w), the Young's moduli observed (CS = 0.85 MPa, SS = 0.92 MPa) were nearly identical for two elastomers incubating colloidal and sol–gel silica nanofillers. However, with 20 and 24% (w/w) sol–gel silica loading, fairly higher Young's modulus (20% = 1.83 MPa, 24% = 1.7 MPa) can be recorded for SS–silica nanocomposite in comparison to CS silica (20% = 1.0 MPa, 24% = 0.83 MPa) filled elastomers.

These ductile materials gradually crossed a yield point, point at which the non-linear behavior begins, at some value of stress and gradually deviate from linearity. The ultimate tensile strength (UTS) or tensile strength is the maximum engineering stress value was determined in a tension experiment. The tensile load versus deformation relationship of elastomers is considerably nonlinear. The slope of the curve drops off significantly (curves not shown) and the gradient changes as the elastomer is stretched.[33] A typical result observed for elastomers is a S-shaped stress–strain curve for which Hooke's law is valid only at low strain regime.

The tensile strength of the samples did not change significantly at and below 17% (w/w) of silica loading. However, excitingly near 170% enhancement was recorded for the LSR films made from 20 and 24% (w/w) sol–gel silica dispersions compared to the commercial nanofiller (see Figure 6). Although, the tensile strength of the LSR greatly improved with SS-silica as compared to CS–silica, the elongation properties do not differ much between these two fillers at all experimental loadings tested.

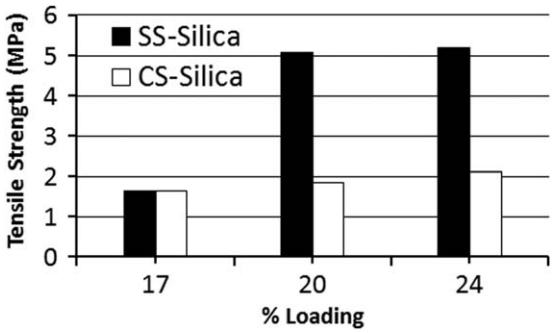

Figure 6. Comparison of tensile strengths of elastomers filled with sol–gel silica (SS–silica) vs. colloidal silica (CS–silica).

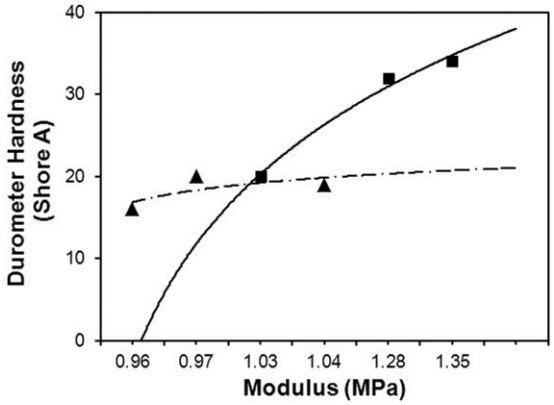

Figure 7. A plot of hardness versus the elastic modulus of LSR samples loaded with SS–silica (solid square) and CS–silica (solid triangle).

This would suggest rather an important phenomenon that one can significantly improve the tensile strength of the LSR by replacing commercial CS–silica with the tailor-made sol–gel silica with no sacrifice on the elongation properties.

Tensile strength largely depends on an elastomer's ability to partially strain crystallize when stretched. With greater crystallization comes increased strength and resistance to stress. The temporary nature of strain crystallization allows elastomers to regain their original shape when the stress is removed. It is observed that the hardness of the sample is a function of modulus. This property can also be correlated with the aggregation state of dispersants within the polymer matrix. The hardness has increased with increasing in modulus for sol–gel silica dispersed LSR material (Figure 7). No significant dependence of the hardness over modulus was observed for the colloidal silica dispersed LSR possibly due to the poor polymer–particle interaction.[34–37]

Hardness is a material's ability to resist indentation under specific test conditions. They could be inherent or processed hardness. The Shore A durometer is a portable device that uses a truncated cone indenter point and a calibrated steel spring to measure the resistance of the elastomer to indentation. The elastomers reinforced with 17% (w/w) sol–gel silica nanostructure showed a hardness of 20. To arrive at the same hardness of 20 it requires 24% (w/w) colloidal silica. When 24% (w/w) loading of sol–gel silica was used the hardness enhanced to 32. Overall, the sol–gel silica provided a greater hardness compared to commercial silica fillers as well under the same loading.

CONCLUSIONS

Beneficial role of mesoscale network morphology of tailor-made silica nanofillers is identified and explored over particulate aspect of commercial nanosilica to reinforce silicone rubber, a class of specialty polymers nanocomposite. The mechanical properties of the elastomer sheets were strongly dependent on the concentration and global morphological state of the particle fillers used. The "*in situ*" formed nanosilica network morphology of sol–gel nanosilica imparts efficient stress bearing ability on the LSR. The dispersion of the interconnected silica assembly (SS–silica) in reactive poly(dimethylsiloxane) nanocomposite, prior to curing LSR, most probably causes a semi-interpenetrating network formation and hence the property enhancement as compared to those evaluated for the commercially available colloidal silica (CS–silica).

Thus, the interconnected tailor-made silica particulate networks offer a suitable replacement for fumed silica to remarkably reinforce mechanical properties for LSR sheets with no compromise on elongation when enforced into PDMS chains at and above 20% (w/w) compared to the commercial colloidal silica under identical conditions.

ACKNOWLEDGMENTS

The authors acknowledge Dr. Hans Rafael Winkelbach and Juergen Ackermann for valuable discussions.

REFERENCES

1. Treloar, L. R. G. The Physics of Rubber Elasticity, 3rd ed.; Clarendon Press: Oxford, **1975**.
2. Mark, J. E.; Erman, B. Rubber-like Elasticity: A Molecular Primer, 2nd ed.; Cambridge University Press: Cambridge, **2007**.
3. Bhowmick, A. K.; Stephens, H. L. Handbook of Elastomers; Marcel Dekker: New York, **2001**.
4. Clarson, S. J.; Semlyen, J. A. Siloxane Polymers; Prentice Hall: Englewood Cliffs, NJ, **1993**.
5. Warrick, E. L.; Pierce, O. R.; Polmanteer, K. E.; Saam, J. C. *Rubber Chem. Technol.* **1979**, *52*, 437.
6. Mark, J. E. *Acc. Chem. Res.* **2004**, *37*, 946.
7. Zheng, P.; McCarthy, T. *J. Langmuir* **2010**, *26*, 18585.
8. Hanley, T. L.; Burford, R. P.; Fleming, R. J.; Barber, K. W. *IEEE Electr. Insul. Mag.* **2003**, *19*, 13.
9. Marciniec, B. Hydrosilylation: A Comprehensive Review on Recent Advances; Springer: London, **2009**.
10. Marciniec, B. Comprehensive Handbook on Hydrosilylation; Pergamon Press: Oxford, **1992**.
11. Roy, A. K. *Adv. Organomet. Chem.* **2007**, *55*, 1.
12. Chujo, Y.; Ihara, E.; Ihara, H.; Saegusta, T. *Macromolecules* **1989**, *22*, 2040.
13. Lewis, L. N.; Stein, J.; Gao, Y.; Colborn, R. E.; Hutchins, G. *Platinum Met. Rev.* **1997**, *41*, 66.
14. Delebecq, E.; Hermeline, N.; Flers, A.; Ganachaud, F. *ACS Appl. Mater. Interfaces* **2012**, *4*, 3353.
15. Demir, M. M.; Menceloglu, Y. Z.; Erman, B. *Macromol. Chem. Phys.* **2006**, *207*, 1515.
16. Cohen Addad, J.-P. *Surf. Sci. Ser.* **2000**, *90*, 621.
17. Schmidt, D. F.; Giannelis, E. P. *Chem. Mater.* **2010**, *22*, 167.
18. Schmidt, D. F.; Cl_ement, F.; Giannelis, E. P. *Adv. Funct. Mater.* **2006**, *16*, 417.
19. Pradhan, B.; Srivastava, S. K.; Ananthakrishnan, R.; Saxena, A. *J. Appl. Polym Sci.* **2011**, *119*, 343.
20. Kickelbick, G. *Prog. Polym. Sci.*, **2003**, *28*, 83.

21. Strat, D. L.; Dalmas, F.; Randriamahefa, S.; Jestin, J.; Wintgens, V. *Polymer*, **2013**, *54*, 1466.

22. Paul, D. R.; Mark, J. E. *Prog. Polym. Sci.*, **2010**, *35*, 893.

23. Iijina, M.; Omori, S.; Hirano, K.; Kamiya, H. *Adv. Powder Technol.* **2013**, *24*, 625.

24. Yilgor, E.; Eymur, T.; Kosak, C.; Bilgin, S.; Yilgor, I.; Malay, O.; Menceloglu, Y.; Wilkes, G. L. *Polymer*, **2011**, *52*, 4189.

25. Joshi, V.; Srividhya, M.; Dubey, M.; Ghosh, A. K.; Saxena, A. *J. Appl. Polym. Sci.* **2013**, *130*, 92.

26. Cohen-Addad, J. P.; Roby, C.; Sauviat, M. *Polymer* **1985**, *26*, 1231.

27. Saxena, A.; Fujiki, M.; Naito, M.; Okoshi, K.; Kwak, G. *Macromolecules* **2004**, *37*, 5873.

28. Fujiki, M.; Saxena, A. *J. Polym. Sci. A Polym. Chem.* **2008**, *46*, 4637.

29. Warrick, E. L. US Patent 2,541,137, **1951**.

30. Wang, H.; Bai, Y.; Liu, S.; Wu, J.; Wong, C. P. *Acta Mater.* **2002**, *50*, 4369.

31. Barthel, H.; Rosch, L.; Weis, J.; Weis, N. A. J., Eds. Fumed Silica Production, Properties, and Applications; VCH: New York, **1996**, p 761.

32. Kumar, S.; Tiwari, S.; Nagaralli, B.; Gupta, S.; Srikanth, A.; Steinberger, H.; Saxena, A. *Rubber World* **2009**, *240*, 25.

33. Powell, P. C. Engineering with Polymers; Chapman & Hall: London, **1983**.

34. Landry, C. J. T.; Coltrain, B. K.; Brady, B. K. *Polymer* **1992**, *33*, 1486..

35. Laridjan, M.; Lafontaine, E.; Bayle, J. P.; Judeinstein, P. *J. Mater. Sci.* **1999**, *34*, 5945.

36. Petrovic, Z. S.; Javni, I.; Waddon, A.; Banhegyi, G. *J. Appl. Polym. Sci.* **2000**, *76*, 133.

37. Luna-Xavier, J.-L.; Guyot, A.; Bourgeat-Lami, E. J. *Colloid Interface Sci.* **2002**, *250*, 82.